Don't work too hard: subsampling leads to efficient analysis of large acoustic datasets

Mike Levine[1] and Alex De Robertis[1]

[1] Alaska Fisheries Science Center, National Marine Fisheries Service, National Oceanic and Atmospheric Administration, 7600 Sand Point Way NE Seattle, WA 98115, USA

Declarations of interest: none

Funding: This research did not receive any specific grant from funding agencies in the public, commercial, or not-for-profit sectors.

Abstract

Echo-integration measurements have been traditionally made from dedicated fisheries survey vessels, but extensive measurements from moorings, autonomous vehicles, and fishing vessels are increasingly available. Processing these data by traditional means developed for well-staffed fisheries surveys can be prohibitively time-consuming, which has limited their use. Automated processing methods exist to efficiently handle these large datasets; however, as compared to post-processing by trained analysts, these methods require substantial expertise and methodological development, and they often produce less certain results. Here, we evaluate the use of subsampling, which takes advantage of the spatial correlation common in many fish populations, to improve the efficiency of traditional processing methods while retaining a high level of precision. We subsampled data from an eastern Bering Sea walleye pollock (*Gadus chalcogrammus*) acoustic-trawl survey and compared estimates of pollock backscatter from subsamples to those from the full survey. Over a survey-wide scale, processing < 5% of the data

resulted in estimates within 5% of those from processing the full survey. This suggests that in some applications there may be diminishing returns associated with exhaustively processing large spatially correlated datasets. We present an example that applies this simple approach by subsampling archived echosounder data from chartered fishing vessels to prioritize the areas surveyed in future surveys, which would not have been feasible without subsampling. When averaged values over large scales (e.g. over a survey domain) are required, precise echo integration estimates can be obtained with modest effort by processing relatively small subsamples of a dataset.

Keywords: Acoustic data analysis, acoustic trawl surveys, subsampling, walleye pollock

1. Introduction

Acoustic surveys are regularly used to assess the distribution and abundance of pelagic fishes and zooplankton over large spatial areas (Simmonds and MacLennan 2005). Traditionally, acoustic backscatter from fish has been measured from dedicated survey vessels, but backscatter measurements are proliferating on an increasing number of acoustic platforms. Acoustic data collected by fishing vessels are increasingly being used to extend survey efforts to under-sampled times and locations (Barbeaux et al. 2017; Fässler et al. 2016; Honkalehto et al. 2011; Honkalehto et al. 2017). Autonomous platforms including unmanned vehicles and moored echo sounders are being used to increase the spatial and/or temporal range of surveys (Brierley et al. 2006; De Robertis et al. 2018, Mordy et al. 2017), and to study the timing and duration of spawning (Kaltenberg et al. 2010; De Robertis et al. 2018) and diel vertical migration behavior (Kaartvedt et al. 2009). Large acoustic datasets are also available from online archives (Wall et al. 2016). While the increase in data availability has benefitted investigations of fish and zooplankton distribution, abundance and behavior, it has led to an increase in the volume of data to be processed. The inability to efficiently process these data often limits their utility (Wall et al. 2016).

A primary goal in processing acoustic backscatter for biological studies is to assign the observed acoustic backscatter to species or species group. Traditionally, analysts accomplish this by interpreting backscatter viewed as echograms (i.e. based on scattering strength, depth distribution, school morphology) in conjunction with information from nearby trawl or optical samples as well as historical distributions of the species in question (reviewed in Horne 2000; McClatchie et al. 2000; Simmonds and MacLennan 2005; ICES 2015b). Analyst review also ensures that artifacts including echoes from the seafloor, bubbles swept under the transducer, and noise spikes are not present in echograms, or that these artifacts are removed so that they do not bias echo integrations (Ryan et al. 2015). Where schools are located near the seafloor or surface boundaries, analyst judgment can be helpful in separating backscatter from fish or invertebrates from that associated with the boundary (ICES 2015b). While these post-processing methods are well-established and effective, they were developed in the context of well-staffed, survey-vessel based, acoustic-trawl surveys, and this type of processing may be too time consuming for other applications.

A pragmatic approach to rapidly processing acoustic data may lie in the geographic structure of fish distributions. Positive spatial autocorrelation, a general property in which ecological variables tend to have increased similarity at shorter distances (Rossi et al. 1992; Legendre 1993), is common in many fish populations. This is likely because fish tend to form geographically continuous schools and because important environmental factors (i.e. water temperature) are also spatially autocorrelated (Kleisner et al. 2010). In the eastern Bering Sea of Alaska (EBS), where the current study is focused, walleye pollock (*Gadus chalcogrammus*, hereafter referred to as pollock), demonstrate a high degree of spatial correlation: the patch size of EBS pollock is consistently > 20 nautical miles (nmi; 1 nmi = 1.85 km), and often > 50 nmi (Horne and Walline 2005; Walline 2007). In the EBS, pollock aggregations regularly extend for 50-100 nmi (Walline 2007).

Systematic sampling designs, in which transects are evenly spaced from a starting point within a survey area (Cochran 1977), are commonly used in in acoustic-trawl surveys because they provide precise estimates of mean abundance for spatially correlated populations (Simmonds and Fryer 1996, Simmonds and MacLennan 2005). This is especially important in many applications (e.g. abundance surveys), as the primary quantity of interest from acoustic measurements is the mean backscatter associated with a given species or species group over the survey domain, which is proportional to the density of organisms in the area (MacLennan et al. 2002). Importantly, the precision of systematic sampling improves with increased spatial correlation because each sample effectively contains more information (Simmonds and MacLennan 2005). We extend this systematic approach to subsampling acoustic backscatter data collected along the survey trackline, and hypothesize that estimates of average backscatter obtained by processing a small fraction of a large-scale dataset can accurately characterize the mean value along the entire vessel track.

We first compare backscatter estimates obtained from subsampled acoustic tracklines to those obtained from completely sampled tracklines using data from a large-scale acoustic trawl survey in the EBS. This survey was used to investigate two related questions: can processing a small subset of data yield estimates of mean backscatter that are close to those from the full survey, and how does this change with the size of the survey area of interest? We then present an example application where the subsampling approach proved useful. In recent years, water temperatures in the EBS have been warmer, and there have been increased numbers of pollock in shallow water to the northeast of the traditional acoustic trawl survey area (Honkalehto et al. 2018; Stevenson and Lauth 2018). As a result, there has been a desire to extend the spatial coverage of EBS acoustic-trawl surveys to capture more of the population. To aid in planning this survey, we efficiently analyzed subsamples of a large archived dataset from chartered fishing vessels when standard survey data were unavailable. We then used the results to examine which of two proposed areas should be given more priority when extending the spatial coverage of the EBS acoustic survey.

2. Materials and Methods

2.1 Acoustic data sources

The analysis used acoustic data from two fish surveys conducted in Alaska's EBS (Figure 1). The 2016 acoustic trawl survey (subsequently referred to as "AT survey") primarily assessed midwater pollock distribution and abundance on the Bering Sea shelf (Figure 2; Honkalehto et al. 2018). The AT survey is part of a biennial time series in the Bering Sea conducted aboard the NOAA ship *Oscar Dyson*. The survey methods are described in detail in Honkalehto et al. 2018. Briefly, this survey used a systematic transect design with 20 nmi transect spacing, covering approximately 5000 nmi of transect line. Along transects, acoustic backscatter was measured at a ping rate of ~1 s^{-1} using a 38 kHz calibrated Simrad EK60 scientific echosounder. Trawl hauls were regularly conducted to identify the species and size composition of acoustic scatterers, and this information was used to partition acoustic backscatter to species and size classes. As is typical in the EBS AT survey, the trawl catch was dominated by pollock, which accounted for 89.5% of catch by weight in midwater trawls (Honkalehto et al. 2018). *Chrysaora melanaster,* a weakly scattering jellyfish (De Robertis and Taylor 2014), accounted for much of the remainder of the catch (8.2% by weight).

The second acoustic data collection occurred during the 2017 eastern Bering Sea bottom trawl survey (subsequently referred to as “BT survey”). This survey is primarily designed to assess demersal fish and crab stocks, and consisted of bottom trawls at fixed stations centered within 20 nmi × 20 nmi grid cells (Conner and Lauth 2017, Stauffer 2004). In 2017, the survey covered a large fraction of the EBS continental shelf, including much of the AT survey area (Figure 1). The survey was conducted on two chartered commercial fishing vessels which continuously collected acoustic backscatter data with 38 kHz calibrated Simrad ES60 echosounders at a rate of ~1 ping s^{-1}. A subset of these data are used to provide an index of midwater pollock abundance, which is used as a separate time series in the pollock stock assessment model (Honkalehto et al. 2017; Honkalehto et al. 2011; Ianelli et al. 2017).

2.2. AT survey acoustic data analysis

During the AT survey, 38 kHz acoustic data were processed by experienced analysts. As part of this processing, analysts attributed acoustic backscatter to species (Honkalehto et al. 2018). Pollock dominate pelagic fishes in this survey (e.g. Honkalehto et al. 2018), and essentially all the backscatter consistent with midwater and demersal fish aggregations was attributable to pollock. We echo integrated backscatter attributed to pollock in the water column (16 m below the surface to 0.5 m above the sea floor) at a 1 ping horizontal resolution using Echoview software (version 8.04.) This resulted in a measurement of the nautical area scattering coefficient (s_A, m^2 nmi^{-2}, see MacLennan et al. 2002 for a description of acoustic units) attributed to pollock for each ping.

We divided the survey track into various sized segments (subsequently referred to as sub-areas) to explore the effects of survey size on subsample backscatter estimates: 15-nmi sub-areas representing short distances, 180-nmi sub-areas representing the average AT survey transect length, 750-nmi sub-areas representing a moderately sized survey, 1500-nmi sub-areas representing a relatively large survey, and a 5000-nmi representation of the entire EBS AT survey. The spatial location of the sub-area datasets is shown in Figure 3; the total number of datasets and the number of pings that define each sub-area are shown in Table 1. Each dataset consisted of continuous pings ordered sequentially along transect lines; some datasets span multiple transects (Figure 3). The last dataset for a given sub-area often included fewer pings than other datasets within the sub-area. This was because the number of pings in the full AT survey was not equally divisible by the number of pings that defined a given sub-area. In cases where the number of pings in the final dataset was > 50% of the number of pings that define that sub-area, the 'short' dataset was retained as a unique dataset. In cases where the number of pings in the final dataset was <50% of the number of pings that defined the sub-area, it was combined with the previous dataset within the sub-area. The mean s_A of each dataset *d* was then calculated as the mean s_A of all pings *i* in that dataset:

$$\bar{s}_{A,d} = \frac{1}{\ } \underset{=1}{\ } s_{A,\ d}$$

Within each dataset *d*, we then created unique subsamples by sampling contiguous 50-ping segments at regular intervals from a given starting point (i.e. systematic sampling, Cochran 1977; Figure 4a). The 50-ping segment length was chosen because it allowed analysts to clearly and rapidly visualize important features (backscatter strength, aggregation shape, and individual fish targets) and remove artifacts (bottom integrations, surface turbulence, or noise spikes) in echograms during this survey (Figure 4b, Figure 5). At a typical survey speed of 6.2 m/s, a 50-ping unit represents approximately 309 m of trackline. The mean s_A of each subsample *s* was then calculated as the mean s_A of all pings *j* in that subsample:

$$\overline{s_A}_{,s} = \frac{1}{\ }\ \ _{j=1}\ s_{A,js}$$

The difference between the mean s_A estimated from a given subsample (i.e. $\overline{s_A}_{,s}$; orange shaded region in Figure 4b) and all pings in the dataset (i.e. $\overline{s_A}_{,d}$; unshaded region in Figure 4b), referred to as percent error, was then calculated for each subsample *s* as

$$perce\ \ t\ error_{,s} = abs\left(\frac{\overline{s_A}_{,s} - \overline{s_A}_{,d}}{\overline{s_A}_{,d}}\right. \times 100$$

Percent error was used as a metric of subsample precision, with lower percent error indicating higher precision.

To determine the relationship between percent error and subsample size in the AT survey, we subsampled from 1% to 100% of the pings present in datasets in 1% increments. For each dataset and subsampling effort level, we systematically subsampled continuous 50-ping units starting at the first ping in the dataset. Percent error for each subsampling effort level was calculated for three sub-areas: 15-nmi (n = 327 datasets), 180-nmi (n = 28 datasets), and 5000-nmi (n = 1 dataset). To assess the precision of percent error estimates, we estimated 95% confidence intervals by bootstrapping: within each sub-area and subsampling effort level, we resampled percent error values with replacement (n = 5000 iterations), and 95% confidence intervals were estimated by taking the 2.5% and 97.5% percentiles of the resulting distribution. Confidence intervals were calculated for the 15-nmi and 180-nmi sub-areas only; confidence intervals could not be computed for the 5000-nmi sub-area as there was only a single estimate at each subsampling effort level.

Because we were primarily interested in the performance of small subsamples that can be post-processed in a fraction of the time required for traditional analysis, we further focused on two specific levels of effort: subsamples containing 5% and 10% of the pings present in complete datasets. This allowed for 20 unique subsamples per dataset in the case of 5% subsampling (i.e. the full dataset could be systematically sampled from 20 different starting points to create 20 unique subsamples, each containing 5% of the full dataset) and 10 unique subsamples per dataset in the case of 10% subsampling. Percent error of the mean backscatter estimate relative to processing 100% of the pings was then calculated for each dataset and subsample at five sub-area lengths ranging from 15-nmi to 5000-nmi (Table 1).

2.3 BT survey acoustic data analysis

Backscatter data from the BT survey were processed rapidly via subsampling to evaluate the abundance of pollock backscatter in several sectors of the Bering Sea shelf during summer 2017. We were specifically interested in estimating if the amount of pollock backscatter present in the northeastern part of the EBS shelf was sufficient to merit surveying this region in 2018. We prepared a subset of data for efficient analysis by identifying the data to be processed, and automating repetitive tasks where possible. We read the data files, fit and corrected for a periodic ±1 dB systematic error present in ES60 data (Ryan and Kloser 2004), and subsampled continuous 50-ping units from the raw echosounder files using the Echolab MATLAB post-processing toolkit. We obtained two unique subsamples for each survey vessel, with one starting at the first available 50-ping interval (i.e. pings 1- 50) and the second starting at the 10^{th} available interval (i.e. pings 501-550). In both subsamples, we sampled 5% of the total data by spacing 50-ping units sequentially every 1000 pings from the starting point. At a typical vessel speed of 5.1 m/s, a 50-ping unit represents approximately 257 m. Measurements at speeds < 3.1 m/s were then removed to avoid sampling regions where vessels were idle, or when the vessel was trawling, which may influence fish behavior (DeRobertis and Wilson, 2006). The subsampled data were then re-written in the same format as the echosounder files using Echolab. After subsampling pings and removing measurements taken during idle and trawling periods, the resulting files generally contained 2.0% - 3.5% of the pings present in the original data. We imported these files into Echoview and added the lines to be edited by the analyst (seafloor exclusion, surface exclusion, and lines to separate near-surface scattering and pollock regions) in an automated fashion and saved the file for subsequent analyst review.

While targeted trawl or optical sampling to verify acoustic backscatter was not conducted during the BT survey, pollock dominate the EBS midwater environment, and are likely to constitute a large proportion of the observed backscatter consistent with fish aggregations (De Robertis et al., 2010, Honkalehto et al. 2011). Backscatter in subsampled echograms was therefore classified by the analyst as pollock when single targets and aggregations consistent with pollock characteristics were detected and "unidentified backscatter" in all other cases (Figure 5). The analyst reviewed the echograms and identified backscatter consistent with pollock, edited the bottom and surface exclusion lines, and excluded any artifacts. Backscatter in the water column (16 m below the surface to 0.5 m above the sea floor) was echo-integrated at a 0.5 nmi horizontal resolution with a minimum S_v threshold of -70 dB re 1 m^{-1}.

The two BT survey vessels did not travel along fixed transect lines as in the AT survey, and survey effort was not consistent throughout the EBS survey region. To allow for comparisons across the survey region, s_A attributed to pollock was averaged into 20-nmi × 20-nmi cells to obtain a single per-cell measure of pollock backscatter for each 5% subsample. The mean s_A for each cell *c* containing observations *i* was calculated as:

$$\overline{s_A}_{,c} = \frac{1}{} \quad {}_{=1} \quad s_{A,}$$

Because the goal of the BT survey analysis was to inform the allocation of survey effort in large-scale areas of the EBS in future surveys, we then further averaged s_A attributed to pollock within cells into 3 regions: the core survey area covered by the semiannual Eastern Bering Sea acoustic trawl survey (“core EBS”, Region 1, Figure 2), the potential expanded acoustic survey area in the Northern Bering Sea (“NBS extension”; Region 2, Figure 2), and a large area in the EBS that is not currently under consideration for acoustic survey expansion (“EBS shallows”; Region 4, Figure 2). The mean pollock s_A in each survey region *r* containing cells *c* was calculated as:

$$\overline{s_A}_{,r} = \frac{1}{} \quad {}_{c=1} \quad \overline{s_A}_{,c}$$

To assess the precision of the two subsamples at the regional scale, we estimated 95% confidence intervals by bootstrapping: within each subsample and region, we resampled cells with replacement to calculate mean pollock s_A (n = 5000 iterations), and 95% confidence intervals were estimated by taking the 2.5% and 97.5% percentiles of the resulting distribution.

Finally, we compared the relative merits of extending survey efforts into the NBS extension region and a second region under consideration, the Russian Cape Navarin Shelf region ("Russian shelf" Figure 2, Region 3). We obtained pollock backscatter measurements in the Russian shelf from 9 acoustic-trawl surveys that surveyed this region from 1994-2014 (Alaska Fisheries Science Center 1994; Honkalehto et al. 2002, 2005, 2008, 2009, 2010, 2012, 2013; Honkalehto and McCarthy 2015). In the NBS extension region, pollock backscatter measurements were only available from the 2017 BT survey. Within each year and for each region *r* containing cells *c,* we computed the total pollock backscatter *T* (units of m^2) as:

$$T_{,r} = \underset{c\,=\,1}{\quad} \left(\overline{s_A}_{,c} \times A_{,c}\right)$$

where $\overline{s_A}_{,c}$ is the mean s_A for a given cell *c* in region *r*, and $A_{,c}$ is the area of cell *c* in region *r* in nmi^2 (generally 400 nmi^2). The proportion of pollock backscatter present in the NBS extension in 2017 was then expressed as a percentage of the total pollock backscatter in the core EBS in 2017 (Figure 2, Region 1). Similarly, for the 9 years where the Russian shelf (Figure 2, Region 3) was surveyed, the pollock backscatter present in the Russian shelf was expressed as a percentage of the total pollock backscatter in the core EBS.

3. Results

3.1 AT survey

The relationship between precision and subsampling effort was strongly dependent on sub-area length. At short 15-nmi sub-area lengths, processing ~70% of pings was needed to attain 5% percent error (Figure 6). At 180-nmi sub-area lengths, processing ~35% of the pings achieved 5% percent error (Figure 6). At the 5000-nmi scale, processing even 1% of the sub-area was sufficient to achieve a low percent error; processing 10% or more of the pings always resulted in less than 5% percent error (Figure 6). This suggests that analyzing small fractions of a large dataset can produce precise estimates of mean backscatter in a large-scale survey area.

When we focused on 5% and 10% subsamples, the precision of estimates again increased with sub-area length. Both 5% and 10% subsampling efforts poorly estimated mean s_A at 15-nmi sub-area lengths, and exhibited high maximum percent error values (i.e. the poorest agreement within all subsamples; Table 2, Figure 1). At scales >1500-nmi, however, both subsampling efforts precisely estimated mean pollock backscatter. At 1500-nmi sub-area lengths, mean percent error was <5%, and the maximum percent error was less than 15%. At the scale of the entire EBS survey (~5000 nmi), percent error was very low in both the 5% and 10% subsamples, and the maximum error was well under 10% in all cases (Table 2, Figure 7). High percent error values were often associated with subsamples that had relatively low backscatter (s_A < 100 m^2 nmi^{-2}). For example, at the 15-nmi scale, the mean percent error for the lowest 10% of backscatter measurements in the 5% subsample was 51% and the mean percent error for the upper 90% of backscatter measurements was 32%.

3.2 BT survey

Echograms created from 5% subsamples allowed for many of the relevant features used by analysts (e.g. the shape, depth and scattering strength of fish aggregations, individual fish targets) to be clearly visualized and evaluated (Figures 4b, 5). Bottom integrations, backscatter from bubbles swept under the transducer, and noise spikes were also readily apparent and could be easily removed. Subsampled echograms exhibited discrete breaks in the seafloor in areas of rapid depth change, and backscatter occasionally abruptly changed in appearance at the start or end of subsample segments. Generally, processing echograms created from subsampled acoustic backscatter data was not more challenging than processing echograms from complete acoustic backscatter data. It was, however, considerably faster: acoustic backscatter data, subsampled to include 5% of the total data and filtered by vessel speed, could be processed by an analyst ~20 times faster than processing the complete acoustic dataset.

The spatial distribution and amount of backscatter attributed to pollock was consistent between two unique 5% subsamples. When averaged into 20-nmi cells, the subsamples exhibited similar spatial patterns (Figure 8). For example, moderately high backscatter (> 500 m^2 nmi^{-2}) was evident in the southwest extent of the core EBS survey area as well as the shelf west of 170º in the core EBS survey area, and a low backscatter region along the eastern extent of the EBS shallows survey area was also evident in both subsamples. Local high-backscatter “hotspots” were also consistently captured, as seen in a single cell located near the northern boundary of the survey grid (indicated with arrow, Figure 8). On a regional scale, backscatter estimates from the subsamples differed by <6% in the NBS extension and EBS shallows regions and <1.5% in the core EBS region (Figure 9). Bootstrapped 95% confidence intervals for the two subsamples overlapped in every region (Figure 9). The close agreement between subsamples suggests that, at larger regional scales, the mean backscatter computed from the entire dataset was precisely estimated by processing a 5% subset. In addition, patterns in backscatter attributed to pollock from the BT survey qualitatively agreed with patterns in pollock abundance in the previous year's AT survey where survey efforts overlapped, with the exception of a low-backscatter region centered around 170° W that was noted in the BT (but not the AT) survey (compare Figures 2 and 8).

The relative abundance of pollock in the NBS or Russian shelf region was a primary consideration in deciding which area should be prioritized in extending the EBS AT survey. We therefore compared pollock backscatter in the NBS extension region during the 2017 BT survey to that from historical AT surveys in the Russian shelf region. Pollock backscatter in the NBS extension region during 2017 was approximately 8.7% of that in the core EBS region (BT subsample 1 = 8.3%, BT subsample 2 = 8.9%). The proportion of backscatter in the Russian shelf region was highly variable in 9 surveys conducted from 1994-2014 (0.9% - 29.7%, of that in the core EBS region; Figure 10). In 6 of 9 surveys, the proportion of pollock backscatter on Russian shelf was lower than the proportion observed in the NBS extension region in 2017 (Figure 10).

4. Discussion

Small subsamples of acoustic backscatter from an AT survey of walleye pollock yielded precise point estimates of mean backscatter over the moderate to large scales which are relevant to many survey applications, as the primary quantities derived from these surveys are large-scale abundance indices. Walleye pollock represents a widely distributed and spatially correlated fish population (Horne and Walline 2005; Walline 2007). The precision of backscatter estimates from subsampled datasets suggests that, for populations displaying similar characteristics, results comparable to those obtained by completely processing datasets can be attained with less processing effort and that exhaustively processing large datasets results in diminishing returns. Our subsampling approach consisted of two steps: we initially tested the precision of backscatter estimates by comparing point estimates from subsamples to point estimates from a fully sampled dataset, and we then used these results to select appropriately sized subsamples from a previously unprocessed dataset. This approach is general and can be applied to evaluate the merits of this approach for large acoustic datasets collected in other regions or on other species assemblages of interest.

In the 2016 AT survey of walleye pollock, 5% subsample estimates of mean backscatter were generally within 5% of the value from fully sampled datasets at scales >1500 nmi of survey trackline. This is not unexpected: as the length of trackline increased, the total number of 50-ping samples comprising a given subsample increased as well. With an increased number of samples, sampling theory suggests that the sample mean will converge towards the true mean (Cochran 1977). At a scale of 1500 nmi, a 5% subsample comprised 500 evenly spaced 50-ping samples; at the scale of the full 5000 nmi survey, 5% subsamples comprised 1635 50-ping samples. At shorter scales (10's to 100's of nautical miles in the AT dataset), the number of samples obtained in small subsamples was too low to reliably approximate the fully sampled mean in a small area, and sampling >35% of the total acoustic backscatter data would have been necessary to achieve 5% percent error. This negates a primary advantage of subsampling, which is to reduce analyst processing time. At our scales of interest (large survey areas), however, precise point estimates of mean backscatter could be produced with substantially reduced effort.

We then used the results of the AT survey analysis to inform subsampling of the 2017 BT survey. Given that our scale of interest was large (1000's of miles), we processed two 5% subsamples and judged precision by empirically comparing results. Mean backscatter estimates at the regional scale were always within 6% between subsamples, and 95% confidence intervals were well constrained around the mean and similar between subsamples. Given this agreement, we considered these subsamples acceptable for informing planning of future surveys. However, if these two subsamples had shown poor agreement, we could simply have sampled additional fractions of the available data until reaching an acceptable level of precision.

It is important to note that the EBS walleye pollock population may be particularly suited to subsampling. Because EBS walleye pollock populations demonstrate strong spatial correlation (Horne and Walline 2005; Walline 2007) and are the dominant contributor to midwater fish backscatter (De Robertis et al., 2010, Honkalehto et al. 2018), echograms created from small 50-ping segments were sufficient for analysts to visualize relevant characteristics, including individual fish targets as well as school morphology and vertical distribution. In systems with a higher diversity, either in terms of species composition or in terms of the distribution of size classes within a species, subsampling longer ping segments may be necessary for analysts to visualize patterns in echograms. Similarly, if the distribution of species or size classes changes rapidly over small spatial scales, or if the survey domain itself is relatively small in comparison the EBS survey domain, the subsampling effort levels that were effective in the current study (5% - 10% of the available data) may be too low to precisely estimate mean backscatter, and analysis of larger subsamples may be necessary. Fortunately, the efficacy of the approach in a given situation can be readily evaluated by comparing the results from processing data subsamples with those from processing the entire dataset.

In a practical sense, subsampling produced actionable results in the current study. We were able to rapidly process a large existing dataset and make a more informed decision as to the merits of extending the 2018 AT survey into the northern Bering Sea or the Russian shelf. The fraction of pollock backscatter in the NBS extension region, as estimated from the subsampled 2017 BT survey dataset, was greater than the fraction observed on the Russian shelf in most of the past AT surveys, suggesting that a sizeable number of pollock were present in the area. In addition, bottom trawl catches from the 2017 BT survey in the NBS extension region indicated that, as compared to a previous survey in 2010, demersal pollock distribution had shifted northward (Stevenson and Lauth 2018). Finally, the primary goal of the Bering Sea AT survey is to assess pollock distribution and abundance in the US exclusive economic zone, which includes the NBS extension region (Honkalehto et al. 2018). Given the substantial midwater pollock backscatter and demersal pollock catches observed in the NBS extension in 2017, the survey was expanded to the NBS extension region in 2018. Importantly, this decision was made with a reasonable amount of effort: analyzing the entire 2017 BT dataset to assess midwater pollock backscatter would not have been feasible in this application, as it consisted of approximately 11 million pings and actionable and timely results were required. Without an efficient processing method, a more ad-hoc decision would have been made. Preliminary results from the 2018 AT survey indicate that approximately 8.7% of core survey area pollock backscatter was observed in the NBS (Honkalehto pers. comm.). This is similar to the estimate derived from the 2017 BT survey acoustic measurements, where approximately 8.7% of core survey area pollock backscatter was observed in the NBS extension region.

Systematic subsampling of acoustic datasets can be considered an extension of the subsampling that occurs at earlier stages of the data collection process. Acoustic surveys necessarily cover only a small fraction of the total available survey area, and therefore the selected survey locations themselves represent a subsample. Systematic subsampling designs are commonly used to select survey locations in midwater (Simmonds et al. 1992; Simmonds and MacLennan 2005) and riverine (Skalski et al. 1993; Enzenhofer et al. 1998; Xie and Martens 2014) fisheries surveys because they precisely estimate spatially-averaged mean abundance in these systems (Skalski et al. 1993; Simmonds and Fryer 1996; Simmonds and MacLennan 2005; Xie and Martens 2014). Echosounders are often operated at ping rates that are lower than the maximum for unbiased data collection during surveys (ICES 2015a), which can further be considered a form of subsampling. Collecting more data would result in a larger processing burden, but little improvement of the survey estimate.

In applications where traditionally processing datasets can create analysis bottlenecks, an alternative approach to speed analyses has been the development of automated and semi-automated post-processing routines. These routines can be general, classifying backscatter across diverse ecosystems and species, or they can be species- and region- specific. General approaches have been used to classify backscatter into broad classes (i.e "fish", "near-surface bubbles") using probabilistic clustering techniques (Anderson et al. 2007), and to identify midwater sound scattering layers composed of zooplankton and small fishes by characterizing layer extent, thickness, and acoustic properties (Cade and Benoit-Bird 2014; Proud et al. 2015). Regionally focused approaches to classify acoustic backscatter to species or acoustic class have included pattern recognition, which has been successful in automatically classifying multiple Chilean pelagic fish species (Robotham et al. 2010), and integrating knowledge from historical species distribution patterns, which has been used to identify areas of the EBS where backscatter can be attributed to pollock based on depth distributions (Honkalehto et al. 2011).

While these automated and semi-automated methods can be effective, the traditional approach to species classification may be advantageous in many instances. Uncertainty in species identification may be lower with manual classification: it is possible, for example, that approaches relying on historical patterns of distribution and abundance (i.e. geographic locations, aggregation behaviors, environmental associations, vertical distributions) may become less reliable as species distributions and/or behaviors change over time. In cases where species of interest occur in close proximity to near-surface sound scattering layers (as in the current study, see Figure 5), it may also be challenging to automatically distinguish appropriate boundaries. Manual post-processing may also allow for echo integration closer to the bottom and surface boundaries, and for more accurate separation of fish and invertebrate backscatter near these boundaries (ICES 2015b). This is especially important in the current application: the expanded survey region is relatively shallow in comparison to the core survey region, and pollock tend to be distributed closer to the bottom at shallower depths (Kotwicki et al. 2009). Additional scrutiny can also allow for more confidence in excluding the strong seafloor return, which can mask the comparatively weak returns from biological targets, as well as in the removal of artifacts due to surface turbulence and vessel noise spikes. Currently used existing automated approaches (Honkalehto et al. 2011) would have required more conservative integration limits (i.e. backscatter integration to 3m above bottom, as opposed to 0.5 m above bottom), or decreased confidence in near-boundary integrations, limiting the utility of the BT analysis at a depth where pollock were likely to be abundant. Finally, automated pattern-recognition approaches have not yet been developed, tested, and refined for many common survey situations, and may be less effective when applied in conditions that differ from the training datasets used to develop the methods. In many cases, it may ultimately be faster and more effective to simply analyze data subsamples than to invest in developing and validating more sophisticated automated approaches.

In the context of the abundance surveys that have traditionally been a primary focus of fisheries acoustics, the spatially averaged mean is the most relevant metric and subsampling may offer substantial efficiencies with little information loss. In addition, as the use of acoustic data in large-scale ecosystem studies continues to expand (Koslow 2009; Ressler et al. 2014; Stauffer et al. 2015; Proud et al. 2017), subsampling can provide a flexible and rapid way to gain insight from large datasets. Choosing subsample size in future applications will ultimately depend on the scale of interest, the diversity and composition of the scattering populations, and the desired degree of precision. Subsampling offers several advantages: it is straight-forward to implement, one can arrive a provisional estimate of backscatter by processing a small subset, and the impact of subsampling in a particular environment can be readily assessed by analyzing several subsets of a dataset and empirically judging precision. Thus, subsampling should not be overlooked, as this simple and accessible approach is likely to make analysis of the large acoustic datasets that are increasingly becoming common more tractable.

References

Alaska Fisheries Science Center. 1994. Preliminary cruise results: NOAA ship Miller Freeman. Cruise 94-07: Echo integration-trawl survey of walleye pollock in the Bering Sea, 40 p. Unpublished report. Available: Alaska Fisheries Science Center, 7600 Sand Point Way NE, Seattle WA 98115.

Anderson, C.I.H., J.K. Horne, and J. Boyle. 2007. Classifying multi-frequency fisheries acoustic data using a robust probabilistic classification technique. J. Acoust. Soc. Am. **121:** 230-237.

Barbeaux, S. J., D. Fraser, L. W. Fritz, and E. A. Logerwell. 2017. Cooperative Multispecies Acoustic Surveys in the Aleutian Islands. U.S. Dep. Commer., NOAA Tech. Memo. NMFS-AFSC-347, 57 p.

Brierley, A. S., R.A. Saunders, D.G. Bone, E.J. Murphy, P. Enderlein, S.G. Conti, and D.A. Demer. 2006. Use of moored acoustic instruments to measure short-term variability in abundance of Antarctic krill. Limnol. Oceanogr. Methods **4:** 18-29.

Cade, D.E. and K.J. Benoit-Bird. An automatic and quantitative approach to the detection and tracking of acoustic scattering layers. Limnol. Oceanogr. Methods **12:** 742-756.

Cochran, W. G. 1977. Sampling Techniques (3rd ed.). John Wiley and Sons, New York.

Conner, J., and R. R. Lauth. 2017. Results of the 2016 eastern Bering sea continental shelf bottom trawl survey of groundfish and invertebrate resources. U.S. Dep. Commer., NOAA Tech. Memo. NMFS-AFSC-352, 159 p.

De Robertis, A., and C. D Wilson, 2006. Walleye pollock respond to trawling vessels. ICES J. Mar. Sci. **64:**, 63: 514-522.

De Robertis, A., D. R. McKelvey, and P. H. Ressler. 2010. Development and application of an empirical multifrequency method for backscatter classification. Can. J. Fish. Aquat. Sci. **67:** 1459-1474.

De Robertis. A., and K. Taylor. 2014. *In situ* target strength measurements of the scyphomedusa target strength measurements of the scyphomedusa *Chrysaora melanaster*. Fisheries Research **153:** 18-23.

De Robertis, A., R. Levine, and C. D. Wilson. 2018. Can a bottom-moored echo sounder array provide a survey-comparable index of abundance? Can. J. Fish. Aquat. Sci.**75:** 629-640.

Enzenhofer, H.J., N. Olsen, T.J. Mulligan. 1998. Fixed-location riverine hydroacoustics as a method of enumerating migrating adult Pacific salmon: comparison of split-beam acoustics vs. visual counting. Aquatic Living Resources **11**: 61-74.

Fässler, S. M. M., T. Brunel, S. Gastauer, and D. Burggraaf. 2016. Acoustic data collected on pelagic fishing vessels throughout an annual cycle: Operational framework, interpretation of observations, and future perspectives. Fish. Res. **178:** 39-46.

Honkalehto, T., N. Williamson. D. McKelvey, and S. Stienessen. 2002. Results of the echo integration-trawl survey for walleye pollock (*Theragra chalcogramma*) on the Bering Sea Shelf and Slope in June and July 2002. AFSC Processed Report 2002-04, 38 p. Alaska Fish. Sci. Cent., Natl. Mar. Fish. Serv., NOAA, 7600 Sand Point Way NE, Seattle, WA.

Honkalehto, T., D. McKelvey, and N. Williamson. 2005. Results of the echo integration-trawl survey of walleye pollock (*Theragra chalcogramma*) on the U.S. and Russian Bering Sea

Shelf in June and July 2004. AFSC Processed Rep. 2005-05, 37 p. Alaska Fish. Sci. Cent., Natl. Mar. Fish. Serv., NOAA, 7600 Sand Point Way NE, Seattle WA 98115.

Honkalehto, T., N. Williamson, D. Jones, A. McCarthy, and D. McKelvey. 2008. Results of the echo integration-trawl survey of walleye pollock (*Theragra chalcogramma*) on the U.S. and Russian Bering Sea shelf in June and July 2007. U.S. Dep. Commer., NOAA Tech. Memo. NMFS-AFSC-190**,** 53 p.

Honkalehto, T., D. Jones., A. McCarthy, D. McKelvey, M. Guttormsen, K. Williams, N. Williamson. 2009. Results of the echo integration trawl survey of walleye pollock (*Theragra chalcogramma*) on the U.S. and Russian Bering Sea shelf in June and July 2008. U.S. Dep. Commer., NOAA Tech. Memo. NMFS-AFSC-194**,** 56 p.

Honkalehto, T., A. McCarthy, P. Ressler, S. Stienessen, and D. Jones. 2010. Results of the acoustic-trawl survey of walleye pollock (*Theragra chalcogramma*) on the U.S. and Russian Bering Sea shelf in June - August 2009 (DY0909). AFSC Processed Rep. 2010-03, 57 p. Alaska Fish. Sci. Cent., NOAA, Natl. Mar. Fish. Serv., 7600 Sand Point Way NE, Seattle WA 98115.

Honkalehto, T., P. H. Ressler, R. H. Towler, C. D. Wilson, and 2011. Using acoustic data from fishing vessels to estimate walleye pollock (*Theragra chalcogramma*) abundance in the eastern Bering Sea. Can. J. Fish. Aquat. Sci. **68:** 1231-1242.

Honkalehto, T., A. McCarthy, P. Ressler, K. Williams, and D. Jones. 2012. Results of the acoustic-trawl survey of walleye pollock (*Theragra chalcogramma*) on the U.S. and Russian Bering Sea shelf in June - August 2010 (DY1006). AFSC Processed Rep. 2012-01, 57 p. Alaska Fish. Sci. Cent., NOAA, Natl. Mar. Fish. Serv., 7600 Sand Point Way NE, Seattle WA 98115

Honkalehto, T., A. McCarthy, P. Ressler, and D. Jones. 2013. Results of the acoustic-trawl survey of walleye pollock (*Theragra chalcogramma*) on the U.S. and Russian Bering Sea Shelf in June - August 2012 (DY1207). AFSC Processed Rep. 2013-02, 60 p. Alaska Fish. Sci. Cent., NOAA, Natl. Mar. Fish. Serv., 7600 Sand Point Way NE, Seattle WA 98115.

Honkalehto, T., and A. McCarthy. 2015. Results of the acoustic-trawl survey of walleye pollock (*Gadus chalcogrammus*) on the U.S. and Russian Bering Sea Shelf in June - August 2014 (DY1407). AFSC Processed Rep. 2015-07, 62 p. Alaska Fish. Sci. Cent., NOAA, Natl. Mar. Fish. Serv., 7600 Sand Point Way NE, Seattle WA 98115.

Honkalehto, T. P.H. Ressler, R.H. Towler, N.E. Lauffenburger, S.C. Stienessen, E.T. Collins, A.L McCarthy, and R.R. Lauth. 2017. Acoustic Vessel-of-Opportunity (AVO) Index for Midwater Bering Sea Walleye Pollock, 2014-2015. AFSC Processed Rep. 2017-04, 32 p. Alaska Fish. Sci. Cent., NOAA, Natl. Mar. Fish. Serv., 7600 Sand Point Way NE, Seattle WA 98115.

Honkalehto, T., A. McCarthy, and N. Lauffenburger. 2018. Results of the acoustic-trawl survey of walleye pollock (*Gadus chalcogrammus*) on the U.S. Bering Sea shelf in June - August 2016 (DY1608). AFSC Processed Rep. 2018-03, 78 p. Alaska Fish. Sci. Cent., NOAA, Natl. Mar. Fish. Serv., 7600 Sand Point Way NE, Seattle WA 98115.

Horne, J. K. 2000. Acoustic approaches to remote species identification: a review. Fisheries Oceanography **9:** 356-371.

Horne, J. K., and P. D. Walline. 2005. Spatial and temporal variance of walleye pollock (*Theragra chalcogramma*) in the eastern Bering Sea. Can. J. Fish. Aquat. Sci. **62:** 2822-2831.

Ianelli, J., S. Kotwicki, T. Honkalehto, K. Holsman, and B. Fissel. 2017. Assessment of the wallye pollock stock in the eastern Bering Sea. In: Stock assessment and fishery evaluation report for groundfish resources of the Bering Sea/Aleutian Islands regions. North Pacific Fisheries Management Council, Anchorage, Alaska.

ICES. 2015a. Manual for International Pelagic Surveys (IPS). Series of ICES Survey Protocols SISP 9 – IPS. 92 pp.

ICES. 2015b. Report of the Workshop on scrutinisation procedures for pelagic ecosystem surveys (WKSCRUT), 7–11 September 2015, Hamburg, Germany. ICES CM2015/SSGIEOM:18. 103 pp.

Kaartvedt, S., A. Røstad, T. A. Klevjer, and A. Staby. 2009. Use of bottom-mounted echo sounders in exploring behavior of mesopelagic fishes. Mar. Ecol. Progr. Ser. **395:** 109-118.

Kaltenberg, A. M., R. L. Emmett, and K. J. Benoit-Bird. 2010. Timing of forage fish seasonal appearance in the Columbia River plume and link to ocean conditions. Mar. Ecol. Prog. Ser. **419:** 171-184.

Kleisner, K. M., J. F. Walter, S. L. Diamond, and D. J. Die. 2010. Modeling the spatial autocorrelation of pelagic fish abundance. Mar. Ecol. Progr. Ser. **411:** 203-213.

Koslow, J.A. 2009. The role of acoustics in ecosystem-based fishery management. ICES J. Mar. Sci. **66:** 966-973.

Kotwicki, S., A. De Robertis, P. von Szalay, and R. Towler. 2009. The effect of light intensity on the availability of walleye pollock (*Theragra chalcogramma*) to bottom trawl and acoustic surveys. Can. J. Fish. Aquat. Sci. **66:** 983-994.

Legendre, P. 1993. Spatial autocorrelation: trouble or new paradigm? Ecology **74:** 1659-1673.

MacLennan, D.N., P.G. Fernandes, J. Dalen. 2002. A consistent approach to definitions and symbols in fisheries acoustics. ICES J. Mar. Sci. **59**: 365-369.

McClatchie, S., R. E. Thorne, P. Grimes, and S. Hanchet. 2000. Ground truth and target identification for fisheries acoustics. Fish. Res. **47:** 173-191.

Mordy, C.W., E.D. Cokelet, A. De Robertis, R. Jenkins, C.E. Kuhn, N. Lawrence-Slavas, C.L. Berchok, J.L. Crance, J.T. Sterling, J.N. Cross, P.J. Stabeno, C. Meinig, H.M. Tabisola, W. Burgess, and I. Wangen. 2017. Advances in Ecosystem Research: Saildrone Surveys of Oceanography, Fish, and Marine Mammals in the Bering Sea. Oceanography **30**: 113-115

Proud, R., M.J. Cox, S. Wotherspoon, and A.S. Brierley. 2015. A method for identifying Sound Scattering Layers and extracting key characteristics. Methods Ecol. Evol. **6:** 1190-1198.

Proud, R. M.J. Cox, and A.S. Brierley. 2017. Biogeography of the global ocean's mesopelagic zone. Curr. Biol. **27:** 113-119.

Ressler, P.H., A. De Robertis, and S. Kotwicki. 2014. The spatial distribution of euphausiids and walleye pollock in the eastern Bering Sea does not imply top-down control by predation. Mar. Ecol. Progr. Ser. **503:** 111-122.

Robotham, H., P. Bosch, J. C. Gutiérrez-Estrada, J. Castillo, and I. Pulido-Calvo. 2010. Acoustic identification of small pelagic fish species in Chile using support vector machines and neural networks. Fish. Res. **102:** 115-122.

Rossi, R. E., D. J. Mulla, A. G. Journel, and E. H. Franz. 1992. Geostatistical tools for modeling and interpreting ecological spatial dependence. Ecol. Monogr. **62:** 277-314.

Ryan, T.E., and R.J. Kloser. 2004. Quantification and correction of a systematic error in Simrad ES60 echosounders. In: ICES FAST. Gdańsk. Copy available from CSIRO Marine and Atmospheric Research. GPO Box 1538, Hobart, Australia.

Ryan, T.E., R.A. Downie, R.J. Kloser, and G. Keith. 2015. Reducing bias due to noise and attenuation in open-ocean echo integration data. ICES J. Mar. Sci. **72:** 2482-2493.

Simmonds, E. J., and R.J. Fryer. 1996. Which are better, random or systematic acoustic surveys? A simulation using North Sea herring as an example. ICES J. Mar. Sci. **53**: 39–50.

Simmonds, J., and D. MacLennan. 2005. Fisheries Acoustics: Theory and Practice, 2nd Ed. Blackwell, Oxford, England.

Skalski, J.R., A. Hoffman, B.H Ransom, T.W. Steig. 1993. Fixed-location hydroacoustic monitoring designs for estimating fish passage using stratified random and systematic sampling. Can. J. Fish. Aquat. Sci. **50:** 1208-1221.

Stauffer, B.A., J. Miksis-Olds, J.I Goes. 2015. Cold regime interannual variability of primary and secondary producer community composition in the Southeastern Bering Sea. Sea. PLOS ONE **10(6):** e0131246. doi:10.1371/journal.pone.0131246.

Stauffer, G. (compiler). 2004. NOAA Protocols for Groundfish Bottom Trawl Surveys of the Nation's Fishery Resources. U.S. Dep. Commerce, NOAA Tech. Memo. NMFS-F/SPO-65, 205 p.

Stevenson, D. E., and R.R. Lauth. 2018. Bottom trawl surveys in the northern Bering Sea indicate recent shifts in the distribution of marine species. Polar Biology. https://doi.org/10.1007/s00300-018-2431-1

Wall, C.C., Jech, J.M., and McLean, S.J. 2016. Increasing the accessibility of acoustic data through global access and imagery. ICES J. Mar. Sci. **73**: 2093-2103.

Walline, P. D. 2007. Geostatistical simulations of eastern Bering Sea walleye pollock spatial distributions, to estimate sampling precision. ICES J. Mar. Sci. **64:** 559-569.

Xie, Y., and F.J. Martens. 2014. An empirical approach to estimating the precision of hydroacoustic fish counts by systematic hourly sampling. Fish. Manage. **34:** 535-545.

Acknowledgments

This study would not have been possible without the data collection efforts of many scientists at the Alaska Fisheries Science Center. The AFSC midwater acoustics group and the officers and crew of the NOAA ship *Oscar Dyson* were instrumental in collecting data at sea. The members of AFSC bottom trawl survey group, as well as the captains and crew of the FV *Alaska Knight* and FV *Vesteraalen*, collected and contributed the bottom trawl vessel data used in this study. Rick Towler developed the Echolab MATLAB toolkit that was used in subsampling raw acoustic data. The comments of N. Lauffenburger and T. Honkalehto and two anonymous reviewers improved the manuscript. The findings and conclusions in this paper are those of the authors and do not necessarily represent the views of the National Marine Fisheries Service. Reference to trade names does not imply endorsement by the National Marine Fisheries Service, NOAA.

Tables

Table 1. The number of unique AT survey datasets at each sub-area length, the nominal number of pings per dataset, and the total number of unique subsamples at 5% and 10% subsampling effort for all datasets combined.

Sub-area length (nmi)	Datasets	Number of pings	Number of subsamples	
			5%	10%
15	327	5000	6540	3270
180	28	59,000	560	280
750	7	245,550	140	70
1500	3	500,000	60	30
5000	1	1,635,237	20	10

Table 2. The precision of mean backscatter estimates for 5% and 10% subsampling effort in the AT survey. The mean percent error for each sub-area length and subsampling effort relative to processing the entire dataset was computed for each subsample (see Table 1). The mean percent error over all subsamples is given. The maximum deviation of any single dataset is given in parentheses.

Sub-area length (nmi)	Subsampling effort	
	5%	10%
15	33.7 (946.6)	22.6 (423.3)
180	14.1 (119.0)	8.9 (48.3)
750	8.1 (39.8)	4.6 (14.4)
1500	4.5 (14.2)	2.4 (6.8)
5000	2.2 (6.1)	1.3 (3.2)

Figure 1. Overview of the Eastern Bering Sea shelf study region. The shaded grey area encompasses the 2017 bottom trawl dataset (“BT survey”), black lines indicate transects in the 2016 EBS acoustic-trawl survey dataset (“AT survey”), and the cross-hatched northern area indicates the Russian shelf expansion region.

Figure 2. Detail of the 2016 EBS AT survey and study regions. Region 1 (referred to as “core EBS”) is the core survey area covered in the biennial eastern Bering Sea acoustic trawl survey. Transect lines are divided into 0.5 nmi horizontal intervals; backscatter attributed to pollock is integrated within each 0.5 nmi interval and backscatter is color coded. Region 2 is the potential expanded acoustic survey area periodically sampled by bottom trawl surveys (referred to as “NBS extension”). Region 3 is the potential expanded acoustic survey area in the Russian Navarin Shelf region (referred to as “Russian shelf”). Region 4 is not under consideration for acoustic trawl survey expansion, but is partially sampled by bottom trawl surveys (referred to as “EBS shallows”).

Figure 3. Locations of sub-area datasets created from the 2016 EBS AT survey. The AT survey was divided into smaller sub-areas of approximately **a)** 15-nmi, **b)** 180-nmi, **c)** 750-nmi, and **d)** 1500-nmi; the complete 5000-nmi survey was also included as a dataset. Unique datasets are identified by alternating shades of grey; n refers to the total number of datasets for a given sub-area length.

Figure 4. Illustration of subsampling procedure. **a)** The shaded grey area indicates a dataset of 5000 pings. Vertical black bars indicate boundaries of continuous 50-ping segments. Red bars indicate 50-ping samples taken from the dataset sequentially every 1000 pings. In this example, 250 pings are sampled (5%). **b)** 1000-ping segment with backscatter attributed to pollock in the EBS. Vertical gridlines separate 50 continuous ping segments. The shaded orange region indicates a 50-ping subsample.

Figure 5. Example of an echogram from the BT survey created from a 5% subsample. The near-surface backscatter above green line is attributed to an unidentified mix of plankton and age-0 pollock (“unidentified backscatter”), while the area below the green line indicates backscatter attributed to age 1^+ walleye pollock. This echogram represents 8 hours: after subsampling and filtering for vessel speeds < 3.1 m/s, it consisted of 1600 pings.

Figure 6. Percent error of mean backscatter estimated from AT survey subsamples as a function of sampling effort (i.e. percent of pings sampled). Points above solid grey line are within 10% of the estimate from the full dataset; points above the dotted grey line are within 5%. Vertical lines indicate 95% confidence intervals calculated using bootstrapped samples of mean percent error

at each point for the 15-nmi (n = 327 datasets per point) and 180-nmi (n = 28 datasets per point) sub-areas; confidence intervals could not be computed for the 5000-nmi sub-area as there was a single estimate at each point. Symbols indicate to sub-areas ranging from 15 nmi to 5000 nmi in length.

Figure 7. Boxplots of percent error of mean backscatter evaluated over distances of 15 to 5000 nmi in the AT survey using **a)** 5% of the total pings in the sub-area and **b)** 10% of the total pings in the sub-area. Values below the dotted grey line are within 5% of the estimate from the full sub-area. Numbers within each boxplot indicate the number of samples in a given category. The solid line within each box represents the median percent error. The lower and upper limits of each box represent the first and third quartile, while the whiskers represent 1.5 of the interquartile range and dots are outliers. Note that the y-axis is logarithmic.

Figure 8. Mean s_A in 20 × 20 nmi cells using two 5% subsamples (**a** and **b**) from the 2017 BT survey dataset. Arrows indicate a high-s_A region north of St. Lawrence Island.

Figure 9. Mean s_A estimates from two 5% subsamples within 3 BT survey regions. Region numbers correspond to regions in Figure 2. Error bars correspond to 95% confidence intervals calculated using bootstrapped samples (n = 5000) of the mean s_A within each survey region and subsample.

Figure 10. Pollock backscatter (expressed as a percent of core survey area pollock backscatter) in the Russian shelf area from acoustic-trawl surveys conducted in 1994 - 2014. The dotted black line represents pollock backscatter (expressed as a percentage of core survey area pollock backscatter) in the NBS extension area, as estimated using the mean of two 5% subsamples from the 2017 BT survey.

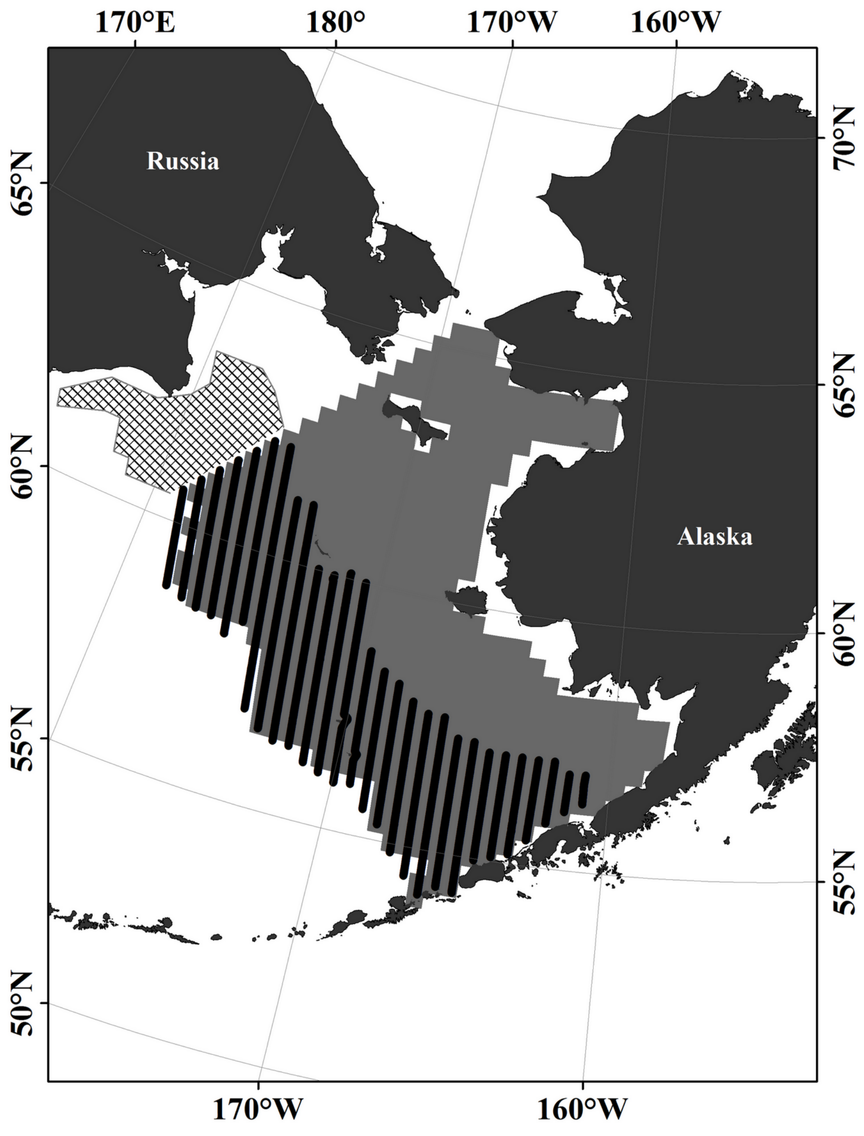

170°E
180°
170°W
160°W
Russia
Alaska
65°N
60°N
55°N
50°N
70°N
65°N
60°N
55°N
170°W
160°W

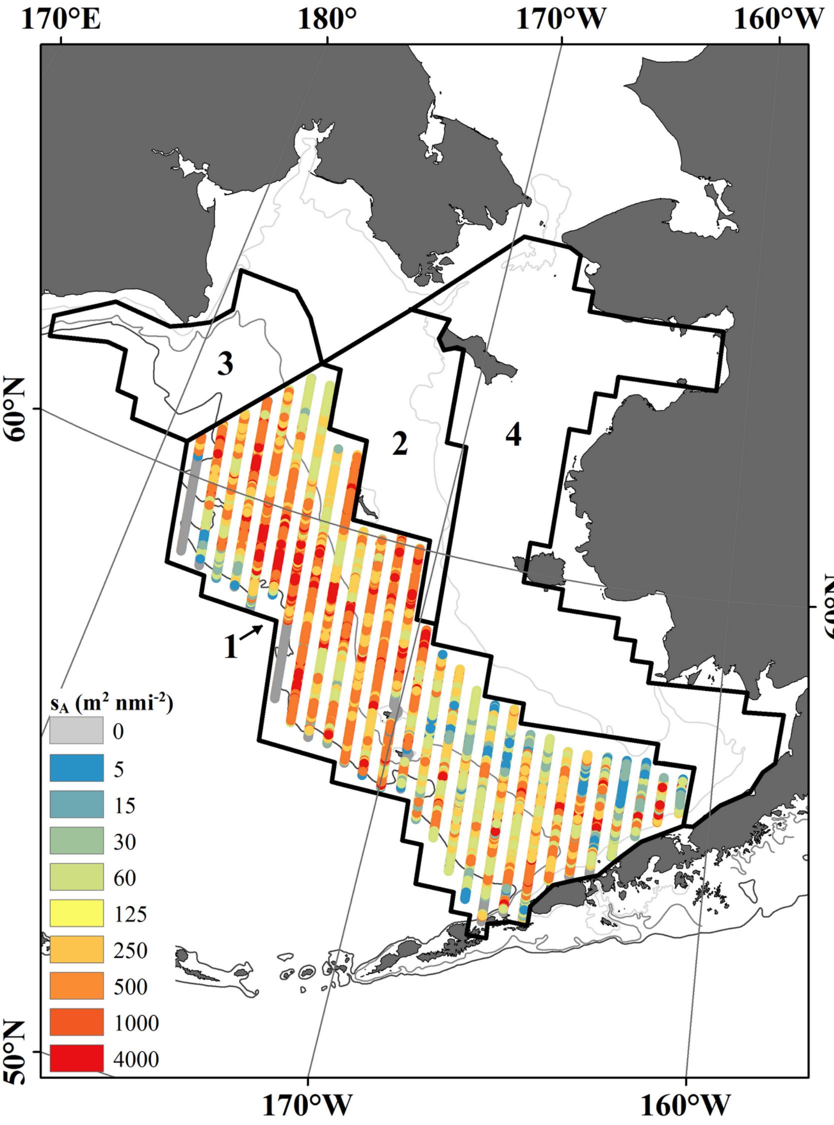

170°E
180°
170°W
160°W
60°N
60°N
50°N
170°W
160°W
3
2
4
1
s_A (m² nmi⁻²)
0
5
15
30
60
125
250
500
1000
4000

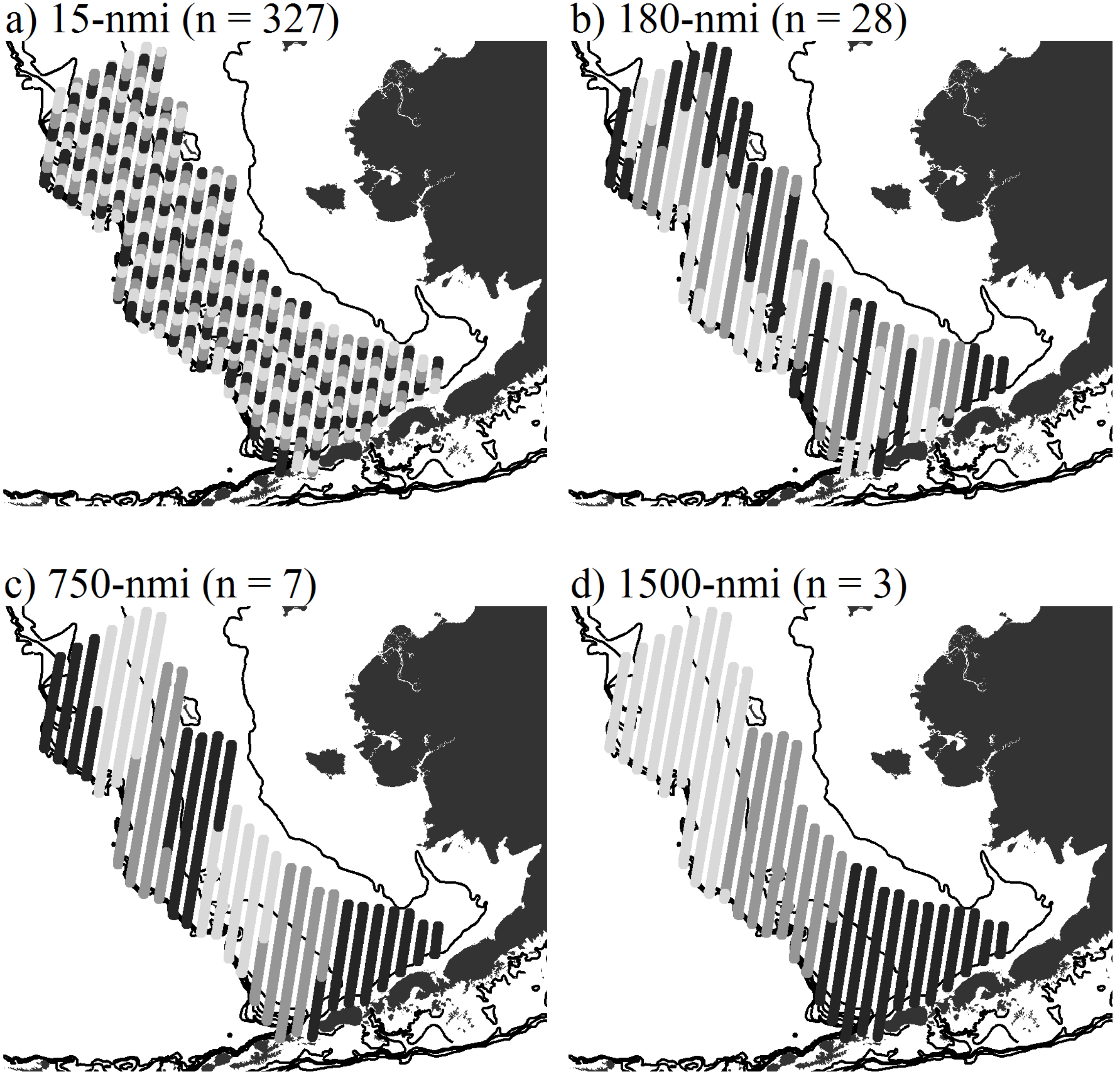

a) 15-nmi (n = 327)
b) 180-nmi (n = 28)
c) 750-nmi (n = 7)
d) 1500-nmi (n = 3)

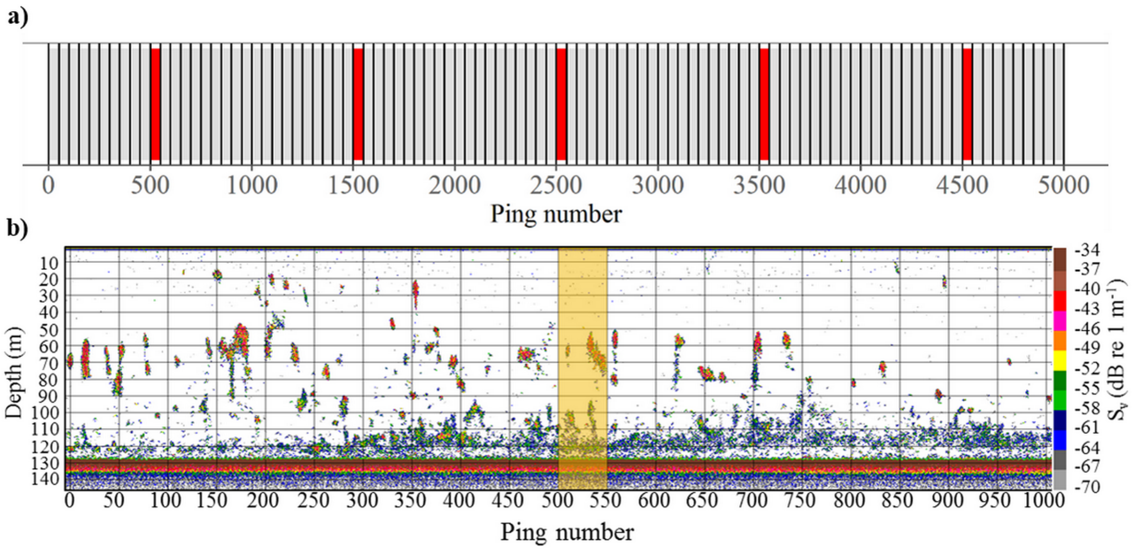
a)
0
500
1000
1500
2000
2500
3000
3500
4000
4500
5000
Ping number
b)
Depth (m)
10
20
30
40
50
60
70
80
90
100
110
120
130
140
0
50
100
150
200
250
300
350
400
450
500
550
600
650
700
750
800
850
900
950
1000
Ping number
-34
-37
-40
-43
-46
-49
-52
-55
-58
-61
-64
-67
-70
S_v (dB re 1 m^{-1})

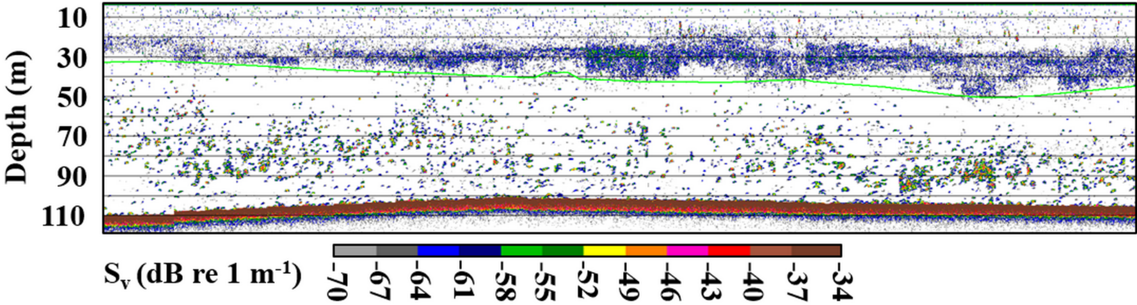

Depth (m)
10
30
50
70
90
110
Sv (dB re 1 m-1)
-70
-67
-64
-61
-58
-55
-52
-49
-46
-43
-40
-37
-34

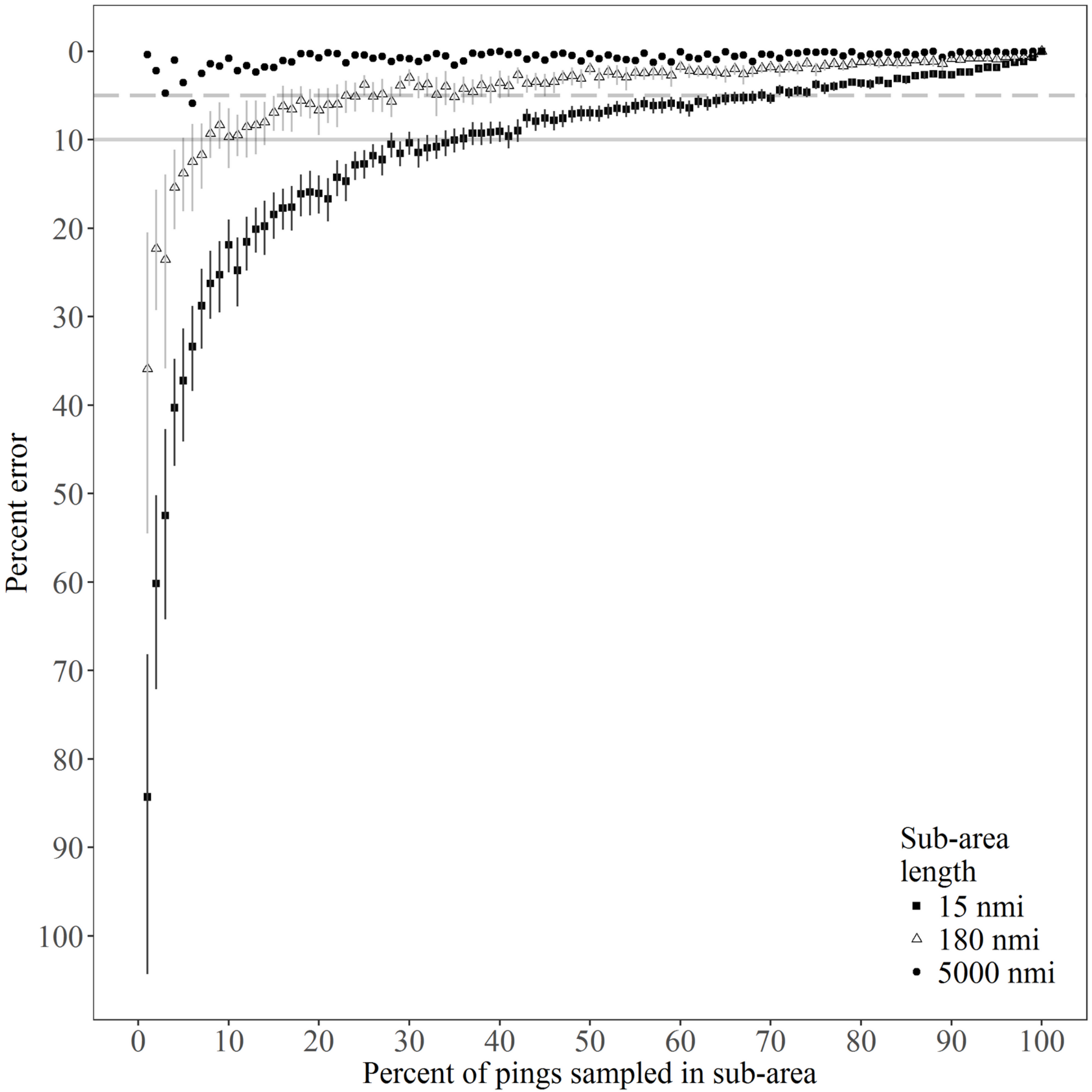

Percent error
0
10
20
30
40
50
60
70
80
90
100
0
10
20
30
40
50
60
70
80
90
100
Percent of pings sampled in sub-area
Sub-area length
15 nmi
180 nmi
5000 nmi

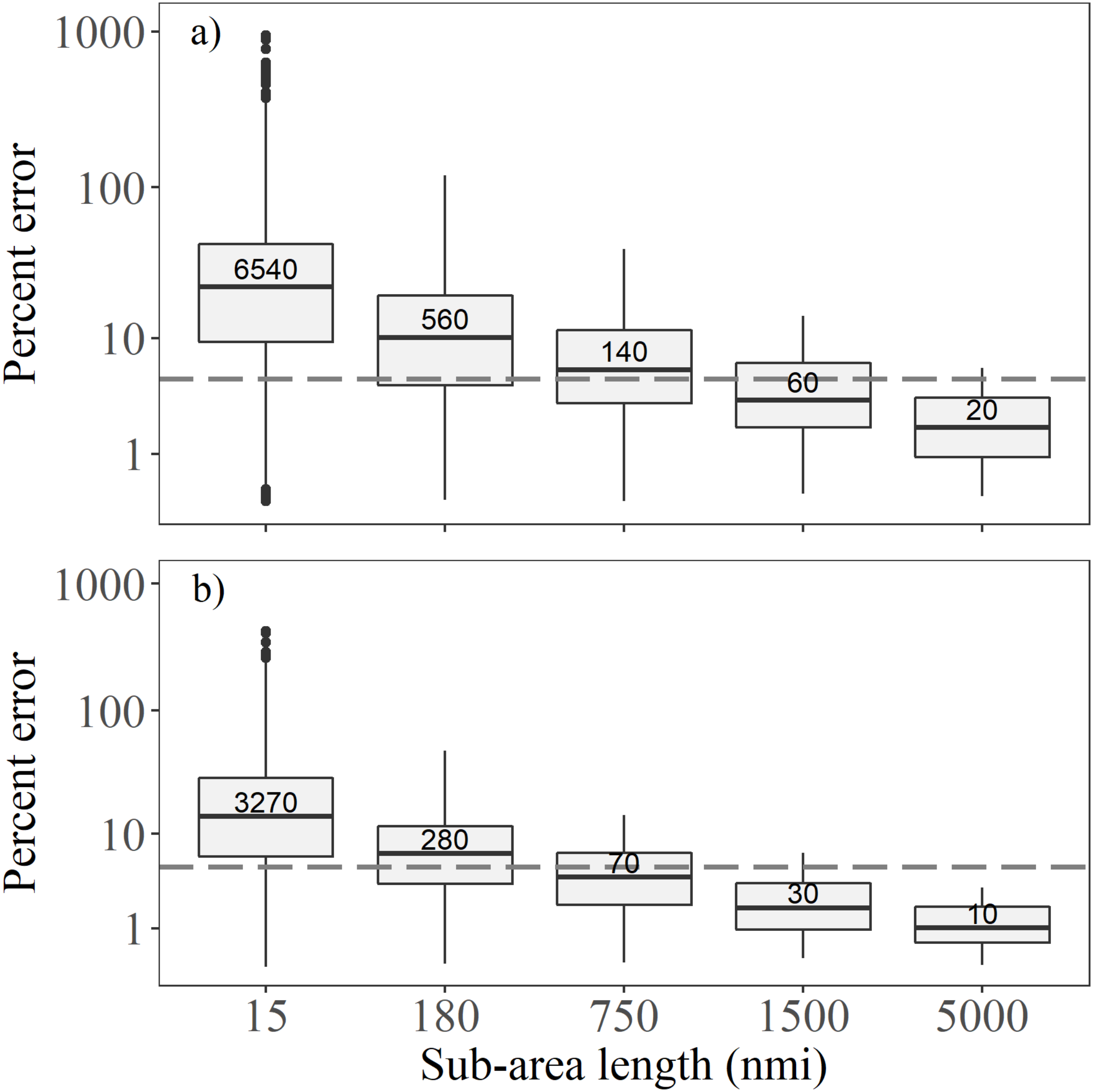
a)
b)
Percent error
Percent error
1000
100
10
1
6540
560
140
60
20
3270
280
70
30
10
15
180
750
1500
5000
Sub-area length (nmi)

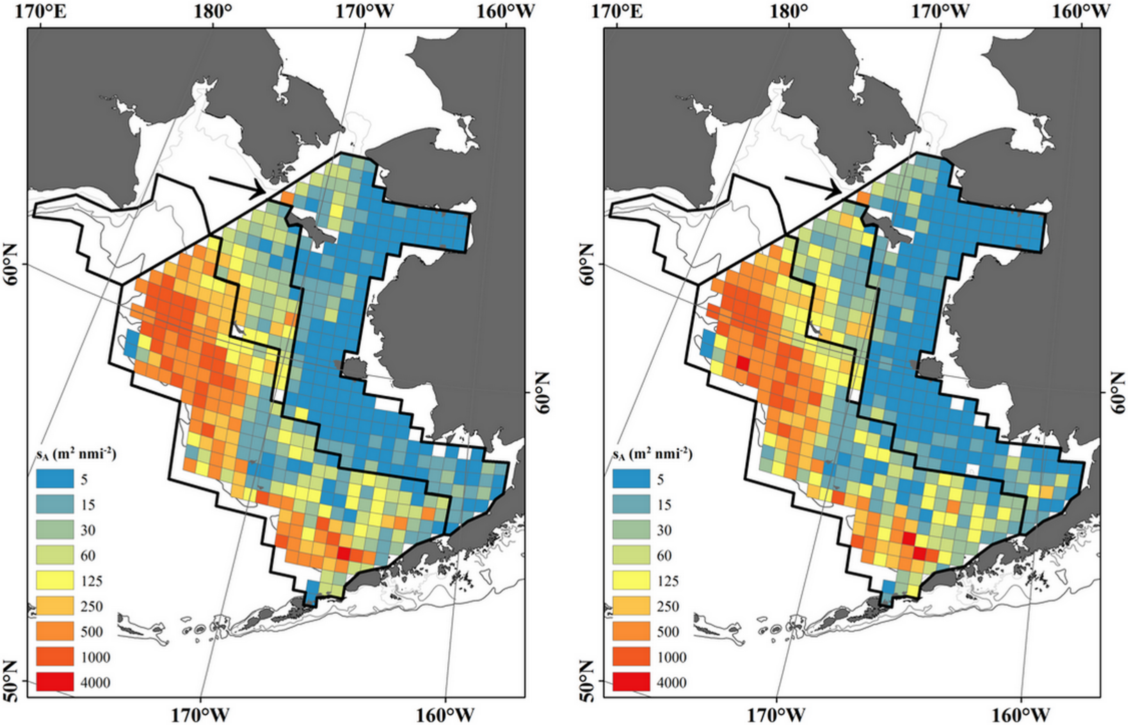
170°E
180°
170°W
160°W
60°N
60°N
50°N
170°W
160°W
s_A (m² nmi⁻²)
5
15
30
60
125
250
500
1000
4000
170°E
180°
170°W
160°W
60°N
60°N
50°N
170°W
160°W
s_A (m² nmi⁻²)
5
15
30
60
125
250
500
1000
4000

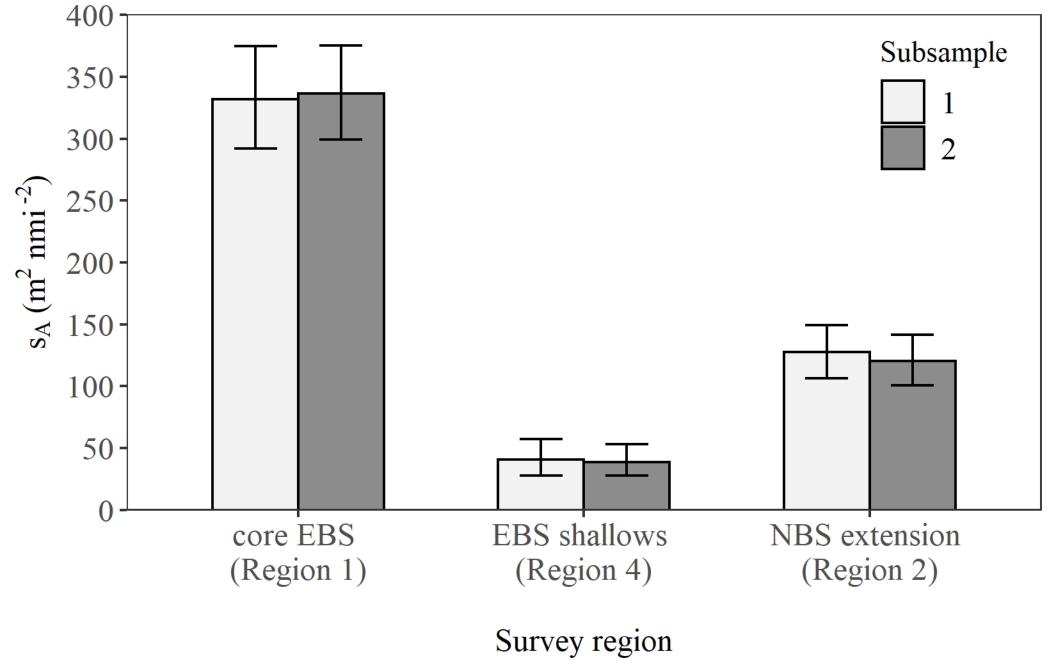

Subsample
1
2
400
350
300
250
200
150
100
50
0
s_A (m^2 nmi^{-2})
core EBS (Region 1)
EBS shallows (Region 4)
NBS extension (Region 2)
Survey region

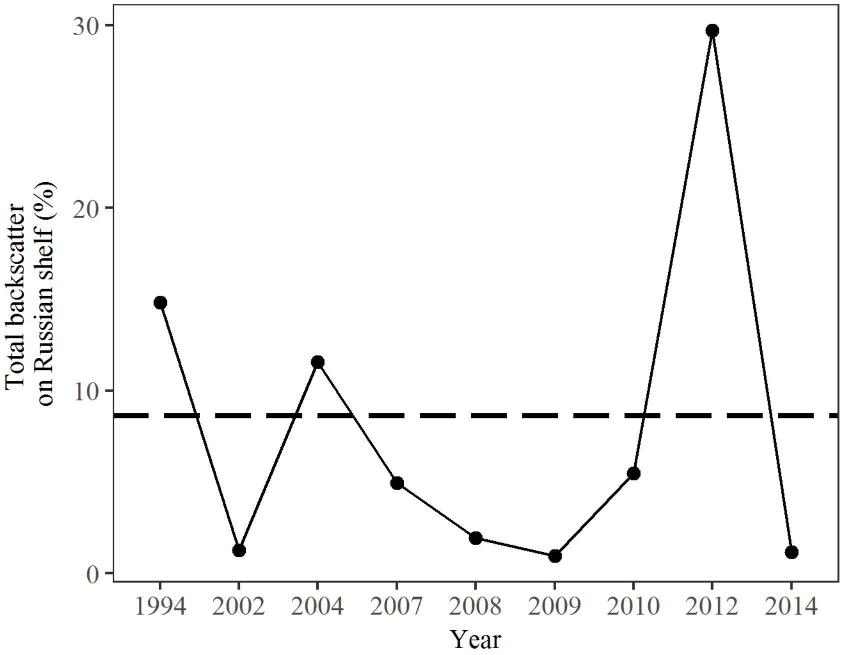
Total backscatter
on Russian shelf (%)
30
20
10
0
1994
2002
2004
2007
2008
2009
2010
2012
2014
Year